communications earth & environment

ARTICLE

https://doi.org/10.1038/s43247-023-01077-w OPEN

Extensive freshened groundwater resources emplaced during the Messinian sea-level drawdown in southern Sicily, Italy

Lorenzo Lipparini [1,2,3]✉, Damiano Chiacchieri[2], Roberto Bencini [4] & Aaron Micallef[1,5]

Deep groundwater resources around the world represent an important potential unconventional source of water. Here we document an extensive (17.3 km^3) fresh/brackish groundwater body preserved in a deep (between 800 and 2100 m) carbonate platform aquifer (Gela Formation.) in southern Sicily (Italy), by using deep well data and a 3D hydrogeological modelling. We attribute the distribution of this fossil groundwater to topographically-driven meteoric recharge driven by the Messinian sea-level drawdown, which we estimate to have reached 2400 m below present sea level in the eastern Mediterranean Basin. The discovery of such an extensive and deep freshened groundwater has significant implications in terms of resource potential for southern Sicily as well as other Mediterranean coastal regions, which share similar geological setting and water scarcity issues.

[1] Department of Geosciences, University of Malta, Msida, Malta. [2] Department of Earth Science, University of Roma Tre, Rome, Italy. [3] Istituto Nazionale di Geofisica e Vulcanologia (INGV), Rome, Italy. [4] Department of Industrial Chemistry, University of Bologna, Bologna, Italy. [5] Monterey Bay Aquarium Research Institute, Moss Landing, USA. ✉email: lorenzo.lipparini@um.edu.mt

Deep groundwater resources are a potential unconventional source of water and potable water that can address water scarcity globally[1]. Fresh and brackish (low salinity) deep groundwater, both from confined and fossil aquifers, have been found onshore and along coastlines down to depths of several kilometers, hosted in both clastic and carbonate aquifers worldwide[2–4]. Examples include the Nubian Sandstone Aquifer across Chad, Egypt, Libya, and Sudan, down to 3500 m[5,6]; the Upper Mega aquifer system of the Arabian platform, at >400 m of depth[7]; the Great Artesian Basin in Australia, down to 2000 m of depth[8]; Tanzania coastal aquifer at 1000 m of depth[9]; the Horn of Africa aquifer at >400 m of depth[10], among others.

The origin of these large deep groundwater systems is considered as due to meteoric water recharge during previous geological epochs, e.g., associated with inter-glacial pluvial periods and lower sea levels, thousands to a million of years ago (e.g., the Nubian Sandstone Aquifer, the Arabian Upper Mega aquifer[4];). Some of them (the Nubian Sandstone Aquifer, the Arabian Upper Mega Aquifer, and the Great Artesian Basin Aquifer) have been exploited for decades for agricultural irrigation, domestic supply, and industry, while others (the Horn of Africa aquifer) are still undeveloped. Also, the offshore, historical drilling on the continental shelf has locally revealed the existence of fresh to brackish groundwater[3,11], in areas such as the east coast of the United States (New Jersey and Florida) and Greenland (associated with widespread ice-sheet during past geological periods), but also e.g., in Suriname, Indonesia, etc. Such offshore groundwaters are usually found at marine depths of less than 100 m and distances of less than 55 km from coastlines[12]. However, in most of the offshore and along coastlines, the current knowledge of these deep aquifers, in terms of fresh to brackish groundwater presence, distribution, volumes, and emplacement mechanisms, is still limited or virtually unexplored.

In this study, we analyze a potential deep carbonate aquifer (the Gela Fm.) preserved in the SE of Sicily (Italy), as it could geologically represent a good calibration for the whole Mediterranean region, of which many coastal areas shared a common recent geological history.

In particular, 6 million years ago, the entire Mediterranean Sea underwent a period of isolation from the global ocean-the Messinian salinity crisis (MSC)[13–15]. During this time, excess evaporation with respect to river runoff and precipitation resulted in >3 km of salt being locally deposited[16]. Two contrasting models explain the origin of this salt. The shallow-water, deep-basin model is based on a sea-level drawdown of 1–4 km from the present-day level, which transformed the Mediterranean Basin into a complex of hypersaline lakes[17–20] (among others). In the alternative deep-water, deep-basin model, salt deposition took place without a substantial sea-level drawdown[21,22] (among others).

As a result, we identified an extensive deeply buried body of fresh/brackish groundwater, hosted in the Gela Fm. carbonates and we demonstrate how the postulated dramatic MSC sea-level drawdown indeed exerted a fundamental control on the emplacement of these deep groundwater, in agreement with the shallow-water, deep-basin model. Specifically, the objectives of our study are to: (i) characterize the geometry, extent, and volume of these deep fresh/brackish groundwater; (ii) assess its origin as due to enhanced topographically-driven flow during the MSC

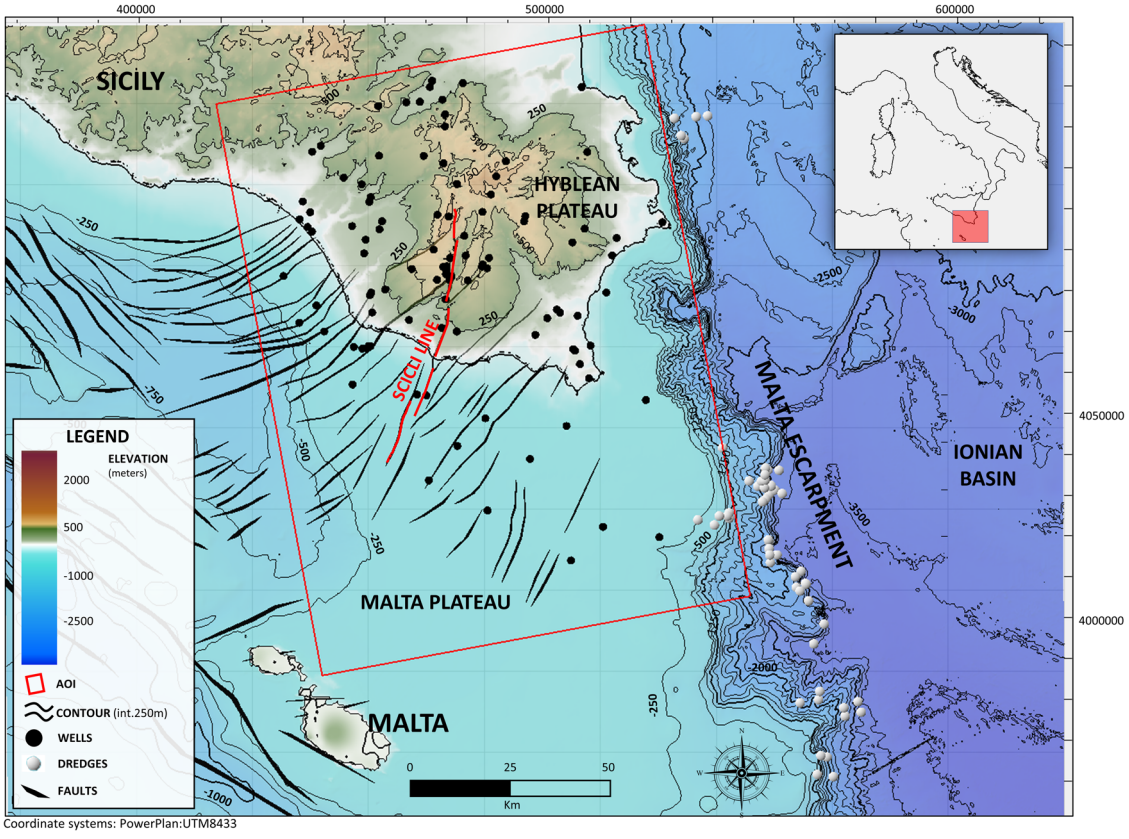

Fig. 1 Study area. Topographic map of the study area (contour interval of 250 m), over the SE of Sicily and the northern Malta Plateau. The 122 wells used in this study are also shown as the location of dredge samples taken along the Malta Escarpment[43,44]. Major faults across the Hyblean Plateau are shown as black polygons (based on seismic interpretation and surface geology at the shallower Ragusa Fm., modified after[37,38]), including the N–S regional strike-slip fault, known as the Scicli line (in red).

sea-level drawdown, (iii) estimate the extent of MSC sea-level drawdown; and (iv) explore implications for groundwater resource potential along the Mediterranean coastline. We address these objectives and knowledge gaps by investigating a large Oil & Gas deep well dataset[23,24]; and by employing 3D geological and hydrogeological modeling.

Results: the Gela Fm. aquifer

Geological framework. The study area covers SE Sicily (Hyblean Plateau) and the Malta Plateau, both belonging to the Pelagian Platform in the central Mediterranean Sea (Fig. 1), which comprise a >5500 m thick sedimentary sequence of Mesozoic to Neogene series (Fig. 2)[25–30].

The oldest series recovered from the Hyblean Plateau (Fig. 2) correspond to Upper Triassic shallow marine platform carbonates of the Gela Formation (Fm.) (also known as Sciacca, Naftia or Taormina Fm.). The Gela carbonate platform was developed over the Pelagian platform since the Norian (Late Triassic). During the Rhaetian time, the onset of a rifting phase[31] unblocked the platform and produced structural highs, where shallow-water carbonate deposition persisted (depositing peritidal dolomites and minor limestones). This was intercalated by higher subsidence sectors over the platform, hosting the deposition of time-equivalent Noto Fm. (interbeddings of laminated micritic limestones and black shales). At the same time, a well-defined and structurally controlled platform margin developed, with the evolution of a subsiding euxinic basin (mainly corresponding to the present-day off-shore areas south of Sicily), filled by the shaly facies of the upper Streppenosa Fm. (micritic limestones and silty mudstones with black shales). Only in the lowermost Jurassic (Hettangian), the Streppenosa basin was completely infilled, and the upper interval of the Streppenosa Fm. (Streppenosa-3) was deposited almost all over the area, including the Gela carbonate platform, which was finally drowned[32].

Shallow marine conditions were locally re-established over the area during early Jurassic time, with the development of isolated carbonate platform limestones of the Siracusa Fm., whereas coeval slope deposit of the Rabbito Fm. and basinal deposit (marls and marly limestones) of the Modica Fm. were deposited. In the middle to late Early Jurassic, a widespread change from shallow marine to basinal deposits is recorded, also marked by the occurrence of volcanic deposits. Pelagic conditions prevailed across the Cretaceous up to the middle Eocene, with the deposition of cherty limestones and marls (Chiaramonte, Hybla, and Amerillo Fms.). From late Oligocene to Miocene, shallow-water carbonate calcarenites and subordinate marl and clays were deposited (Ragusa/Mt. Climiti, Palazzolo and Tellaro Fms.),

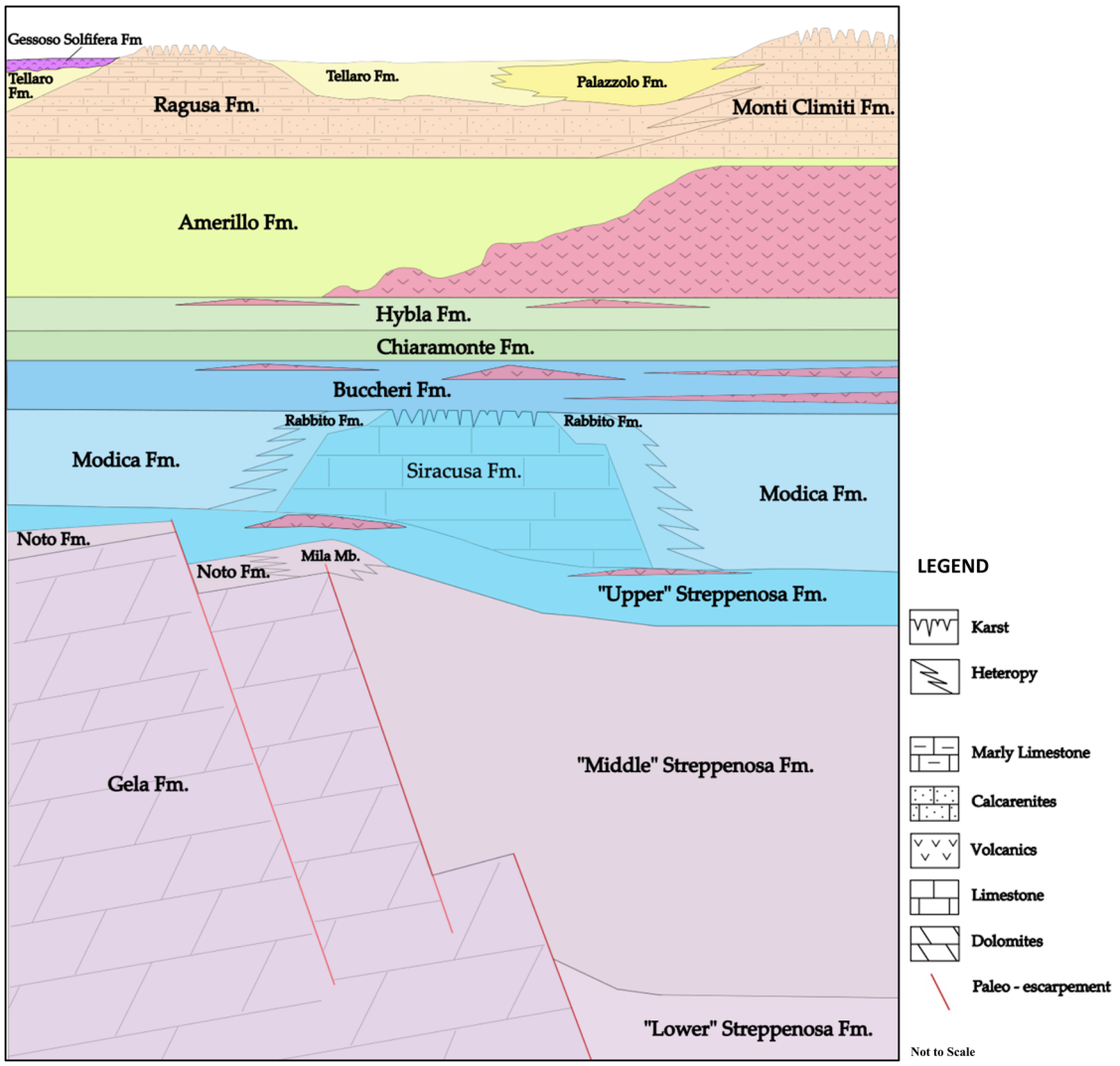

Fig. 2 Stratigraphic scheme of the Hyblean plateau. Main geological formations are shown, with a focus on intervals represented by the Gela Fm., Siracusa Fm., and Ragusa/Mt. Climiti Fms. carbonates.

locally overlain by Messinian evaporites. Offshore, Plio-Pleistocene pelagic deposits cap the sequence.

The fractured late Triassic (Norian to Rhaetian) platform carbonates of the Gela Fm. are known to represent a good quality reservoir for hydrocarbons, while the partially coeval marginal facies of the Mila Mb. and organic-rich shaly Noto and Streppenosa Fms., are known as good seals and source rocks for hydrocarbons[32–35].

At much shallower depths, another carbonate interval is represented by the Oligo-Miocene carbonate unit of the Ragusa Fm., which widely outcrops onshore across the Hyblean Plateau, where it shows extensive karst and fracture systems developed[29,36].

The study area is intersected by a major N–S regional strike-slip fault, known as the Scicli line (Fig. 1), which is a crustal-scale transtensional, near-vertical tectonic feature that is considered to be still active at present-time[37]. A setting of NE–SW normal faults also widely occurs, creating a horst-and-graben framework that cuts through the whole area (Fig. 1)[38].

At present day the main aquifer in the Hyblean Plateau onshore is represented by the outcropping Ragusa Fm. carbonates. Within the upper, more marly, member of the Ragusa Fm. (Irminio Mb.) there is the shallower aquifer at depths of 100–150 m, which is partially confined. A second, deeper and better confined, aquifer is found in the lower calcarenitic member (Leonardo Mb.), approximately 200–400 m deep. In both aquifers, permeability is related to secondary porosity by fracturing, since both carbonates and marls have low inter-granular porosity. Locally, the presence of major regional tectonic structures brings the two aquifers into hydraulic contact and exerts significant hydraulic pressure, which is manifested by the emergence of artesian springs. These aquifers are also controlled by karst dissolution. The development of a karst network along fractures within the Ragusa Fm. began during the late Miocene uplift tectonic phase and continued during Pliocene and Quaternary, when tectonic and eustatic episodes produced two currently well-preserved karst levels in the central sector of the plateau[29]. The only knowledge about deeper aquifers in the study area was the presence of deep fresh/brackish groundwater being detected in an onshore well (Licodia-1) in the Gela Fm., some 700 m below the topographic surface. However, this potential aquifer was never investigated.

3D geometry and structure. Based on the analysis of 121 deep well composite logs (67 of which reached the Gela Fm., Supplementary Table 2) we reconstructed the stratigraphic and structural 3D regional geometry of the Gela Fm. for the whole study area (Methods—3D geometric and structural reconstruction). The structural top of the Gela Fm., in-depth, is shown in Fig. 3

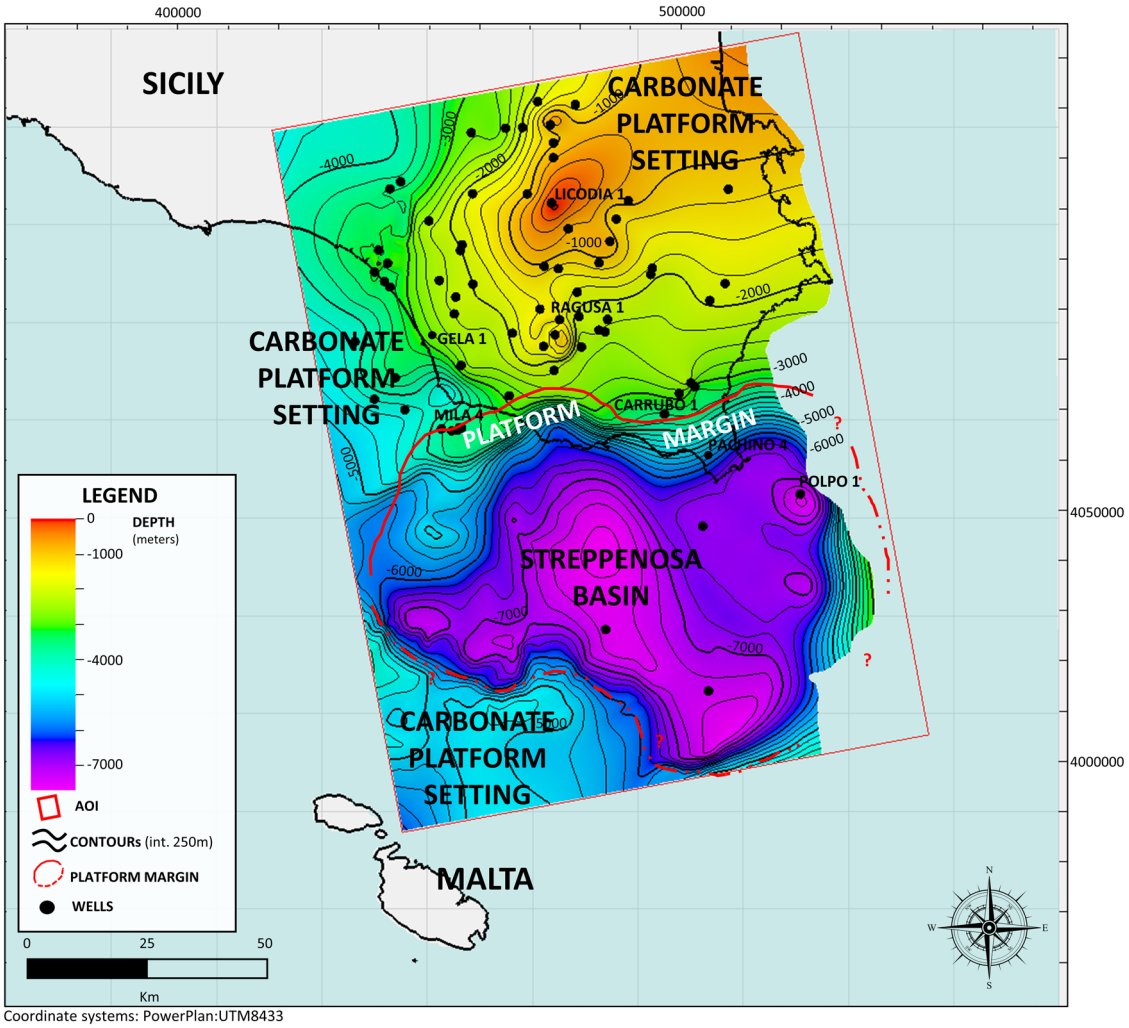

Coordinate systems: PowerPlan:UTM8433

Fig. 3 Structural map of the Gela fm. Map of the structural top surface of the Gela Fm., in-depth (in m msl). The Gela carbonate platform margin is shown as a red continuous (higher confidence) and dotted (lower confidence) line, as a result of more or less well data constraints and supporting documentation from published articles.

(Depths are given with respect to mean sea level/msl, as positive numbers when above sea level, negative numbers when below). The highest portion of the Gela Fm. is at about 140 m msl (at Licodia-1 well, red colors in Fig. 3), still buried 750 m below the topographic surface. Except at that location, the Gela Fm. top surface is located below msl in the whole study area, buried below an average thickness of 2600 m of overburden succession.

The areas at higher elevation at present-time (green to red colors in Fig. 3) mostly correspond to a paleogeographic carbonate platform setting (e.g., at Gela-1, Ragusa-1, Licodia-1 wells) and a platform margin setting (e.g., at Mila-4 and Carrubo-1 wells), while the deeper areas at present-time (purple colors in Fig. 3) correspond to the time-equivalent Triassic basin, known as Streppenosa basin (e.g., at Pachino-4 and Polpo-1 wells).

Groundwater pressures. We analyzed all available pressure data and indicators, obtained from Drill Steam Tests (DSTs), production tests, and mud-weight profiles (Methods—Groundwater pressure analysis). As a result, 31 pressure measurements were obtained, which allowed us to calculate water pressures across the whole study area (Fig. 4). Most of the pressure data are recorded close to the Gela Fm. top., at different absolute depths (−700/−4300 m). Groundwater pressures show a very good linear correlation with depth (Fig. 4a, b), suggesting an overall hydrostatic trend.

Groundwater salinity. We analyzed composite logs, DSTs, and production tests to characterize groundwater salinity (expressed in milligrams per liter—mg/l—of NaCl equivalent; see Methods—Groundwater salinity analysis) within the Gela Fm. (Fig. 5—Methods—Groundwater salinity analysis). Groundwater salinity increases with depth (Fig. 5), varying from fresh (2200 mg/l at −140 m, in Licodia-1 well), to brackish (14,000–20,000 mg/l at −750 m in Monterosso-1 well, at −1340 m in Chiaramonte-1 well and at −1900 m in Rocca-1 wells), down to saline and hypersaline groundwater observed in the deeper structural areas (from 55000 to 100000 mg/l at −2060 m in Vittoria-1 well, at −2865 m in Noto-1 well and at −3360 m in Gela-1 well). It was observed that salinity does not show any relationship with respect to stratigraphic position within the Gela Fm., which suggests a lack of stratigraphic control over its present-day distribution. Most of the fresh/brackish groundwater occurs above a depth of −1400 m, but it extends down to −2100 m.

The distribution of freshened groundwater in Fig. 5 appears elongated following in the same direction as the major tectonic

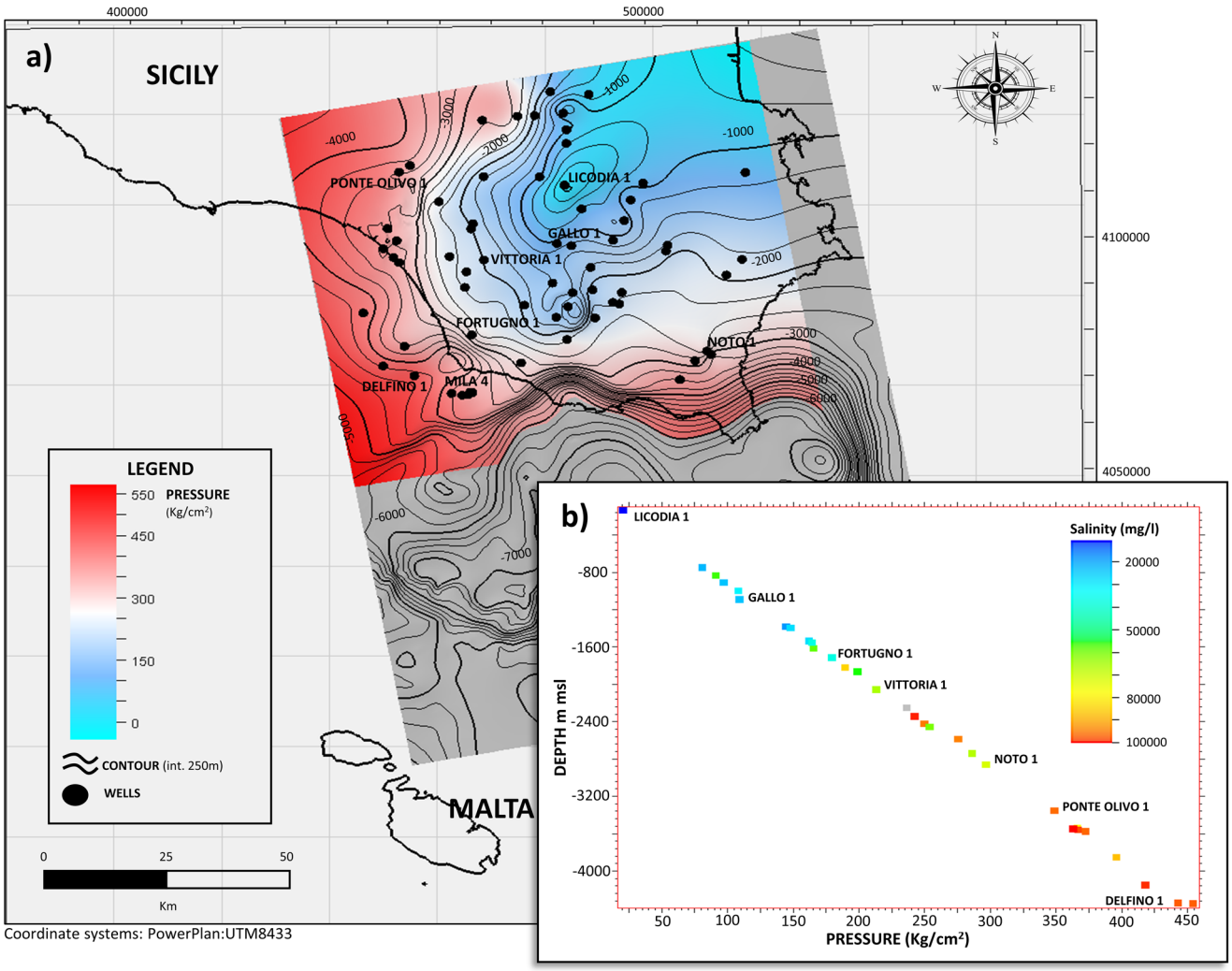

Fig. 4 Groundwater pressure map of the Gela fm. a Groundwater pressure distribution of the Gela Fm., shown over its structural depth map (depths are in m msl). Colors represent groundwater pressure. All well with available pressure data are shown. The key calibration wells are named. **b**) Graph of groundwater pressure versus depth (in m msl) for the Gela Fm. (colors represent salinity).

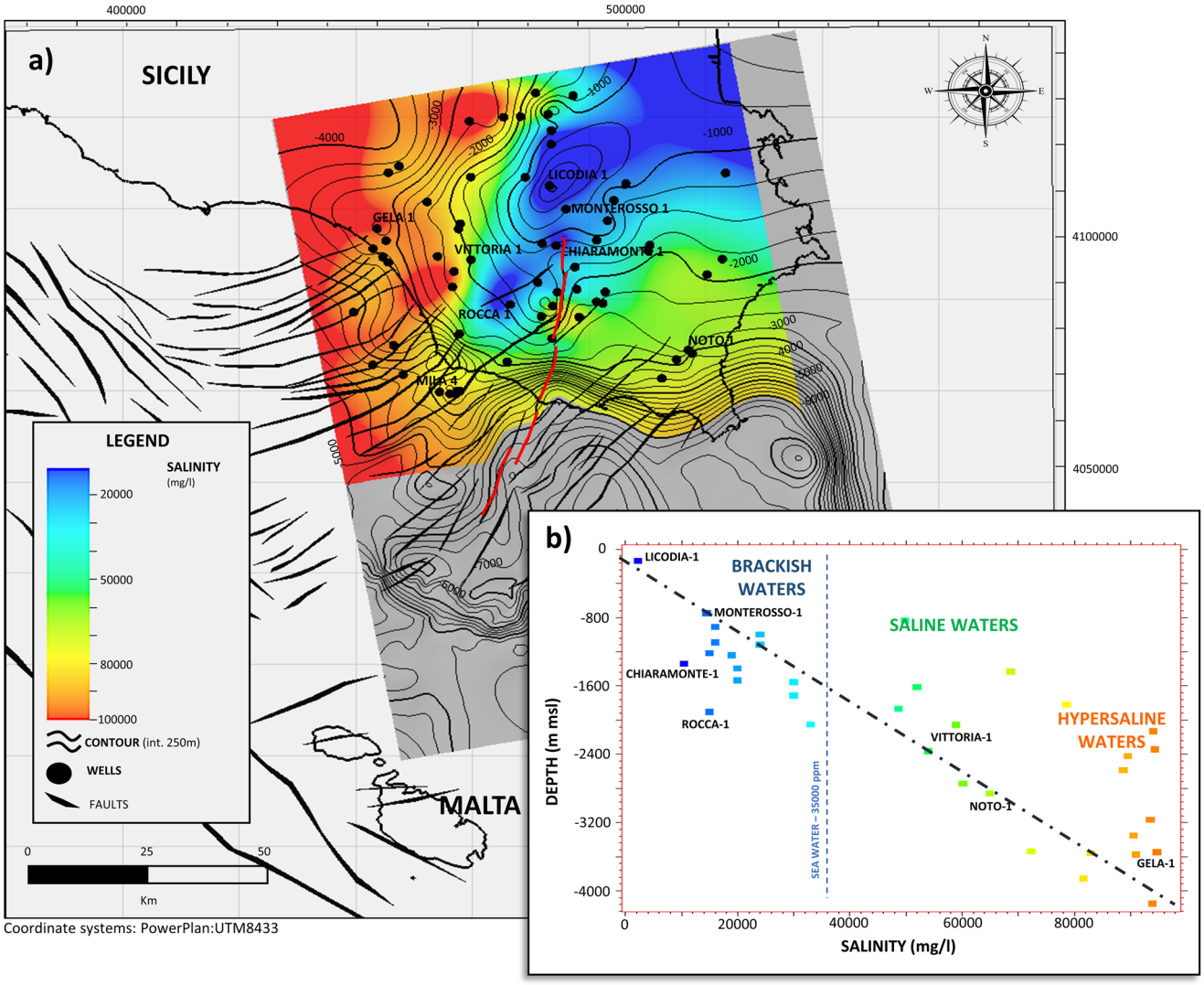

Fig. 5 Groundwater salinity map of the Gela fm. a Groundwater salinity distribution of the Gela Fm., shown over its structural map. Salinity is expressed in parts per million (mg/l) of NaCl equivalent. All well with available salinity data are shown. Major faults across the Hyblean Plateau are also shown including the N-S regional strike-slip Scicli line (in red). **b** Graph of salinity versus depth (m msl) for the Gela Fm. The data show different clusters, from shallower fresh/brackish waters to deeper salty/hypersaline waters. For comparison, present-day seawater salinity (35,000 mg/l) is marked by a dashed blue line.

lineaments across the Hyblean Plateau, such as the N–S trending Scicli Fault and the NE–SW trending Hyblean foreland-related faults, suggesting a possible relationship.

3D modeling and volumetric estimate. To estimate the potential volume of freshened groundwater, we developed a 3D hydro-geological geocellular model for the entire Gela Fm. (Fig. 6 and Methods—3D groundwater model and volumetric calculations).

Based on the resulting 3D property model, a volume of 17.3 km^3 of fresh/brackish groundwater (between 2000 and 20,000 mg/l) is estimated between the top (top of the Gela Fm.) and base (flat surface at 2100 m below present-day sea-level) of the freshened groundwater body (Fig. 6).

Discussion

The identified extensive fresh to brackish groundwater body in our data appears to be trapped on the highest structural culmination of the Gela Fm., (Fig. 5), below the present-day Hyblean Plateau onshore. The recorded linear increase of pressure with depth (Fig. 4), the lack of overpressures and underpressures, and the vertical stratification of groundwater (in terms of salinity, Fig. 6), suggest an overall well-connected aquifer. This implies that the Gela Fm. acts as an excellent regional-scale carbonate aquifer, in view of its large extent and thickness. This is also likely favored by a pervasive fracture porosity system across the whole platform body[33,35], as is frequently the case for shallow-water carbonate platform reservoirs[39,40]. The distribution of freshened groundwater also appears to be controlled by major structures across the Hyblean Plateau, such as the N–S trending Scicli Fault and the NE–SW trending Hyblean foreland-related faults (Fig. 5).

We hypothesize that the occurrence of freshened groundwater down to a depth of −2100 m below present-day sea level can be explained by topographically-driven infiltration of meteoric freshwater enhanced by sea-level drawdown during the MSC. In our conceptual model, the lateral and vertical distribution of the freshened groundwater across the Gela Fm., which has never been meteorically exposed, can be attributed to recharge via an elongated section above its present-day structural culmination (at Licodia-1 well location, Fig. 4), where the thickness of the

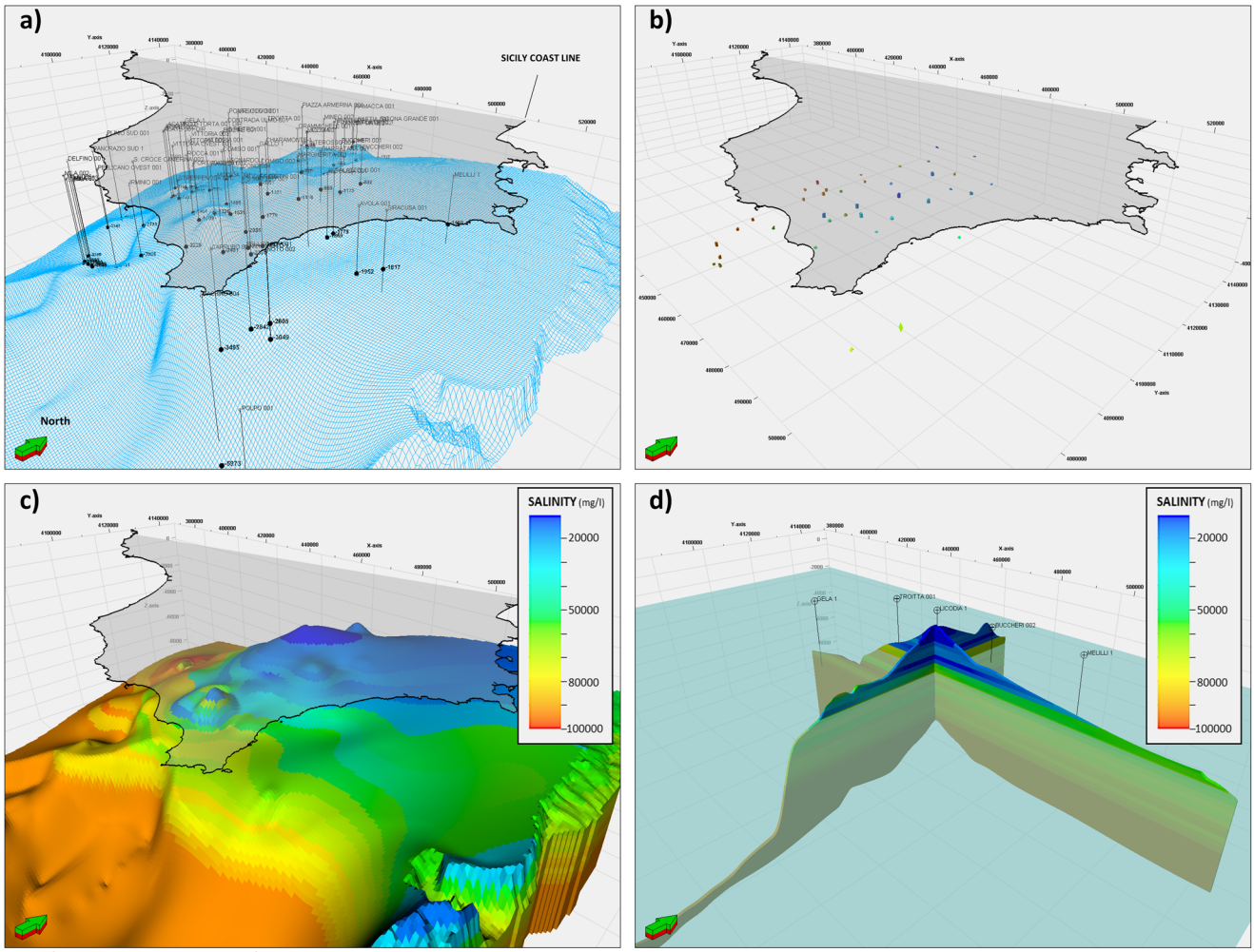

Fig. 6 3D Modeling of the Gela fm. a 3D geocellular grid of the Gela Fm. the top surface, with well data and well tops used to reconstruct its 3D geometry. **b** Upscaled groundwater salinity property cells recorded at well locations in the Gela Fm. **c** Resulting final 3D groundwater salinity property model for the whole Gela Fm. at regional scale; fresh/brackish groundwater is shown in blue/light blue colors, while saline and hypersaline groundwater are denoted by yellow/orange/red colors. **d** East-West and North-South model cross-sections, clearly showing the vertical stratification of salinity with depth; a flat transparent light blue surface is also shown, representing a quite well-defined regional horizontal limit between fresh/brackish (above) and more saline/hyper-saline groundwater (below), at 2100 m below present-day sea-level: this flat limit likely represents, in our hypothesis, a relic of the hypothetical sea-level reached during the MSC. (see also Methods—3D groundwater model and volumetric calculations).

overburden succession corresponds also to its minimum of only 750 m, in comparison to most of the area where an average thickness of 2600 m of the overburden is recorded. This area is moreover strongly influenced by the presence of the N–S Scicli transtensional regional fault and associated fracture systems, which could have enhanced the hydraulic conductivity between the deeply buried Gela Fm. and the shallower Ragusa Fm., which has been exposed since the Late Miocene[36].

To test this hypothesis, the study area was back-deformed to the Messinian (Methods—Back-reconstruction to the MSC), when the uplift of the Hyblean Plateau (foreland) was already happening, as indicated by the onlap of Messinian deposits across the present-day Hyblean Plateau[27]. From the resulting reconstruction (Fig. 7), we infer that freshened groundwater (as observed at present-day) was able to reach the depth of −2400 m below present-day sea-level during the MSC, which can hence be proposed as a first approximation for the sea-level drawdown in the eastern Mediterranean Basin during the MSC.

The inferred value of 2400 m compares well with (i)[18] who estimate a drawdown of 2000 m for the eastern Mediterranean by observing surfaces of erosion in the Nile Delta and based on a model that evaluated water inputs and outputs in the Mediterranean basins; (ii)[13] who suggested a maximum drawdown of ~2400 m in the eastern Mediterranean Basin based on an integrated quantitative model that reproduces the closure of the Atlantic spillway and evaporative drawdown; (iii)[41] who estimated a drawdown of 1800–2000 m in the eastern Mediterranean Sea based on isostatic restoration of the palaeo-shorelines; and (iv)[42] who, using numerical simulations, found that a sea-level drop of 1900 m could explain deposits attributed to the Zanclean megaflood.

For such a scenario to be feasible, a direct hydraulic connection was needed between the observed deep freshened groundwater found in the Gela Fm. aquifer and the Mediterranean Sea waters during the MSC. The Malta Escarpment (Fig. 1) to the east is a likely candidate for such a direct connection, as the Gela Fm. there is considered to outcrop at sea, based on the reconstructed geometrical 3D regional model (Methods—3D geometric and structural reconstruction, Fig. 8) and dredge samples from the Malta Escarpment[43,44] (Fig. 1), in agreement with reconstruction

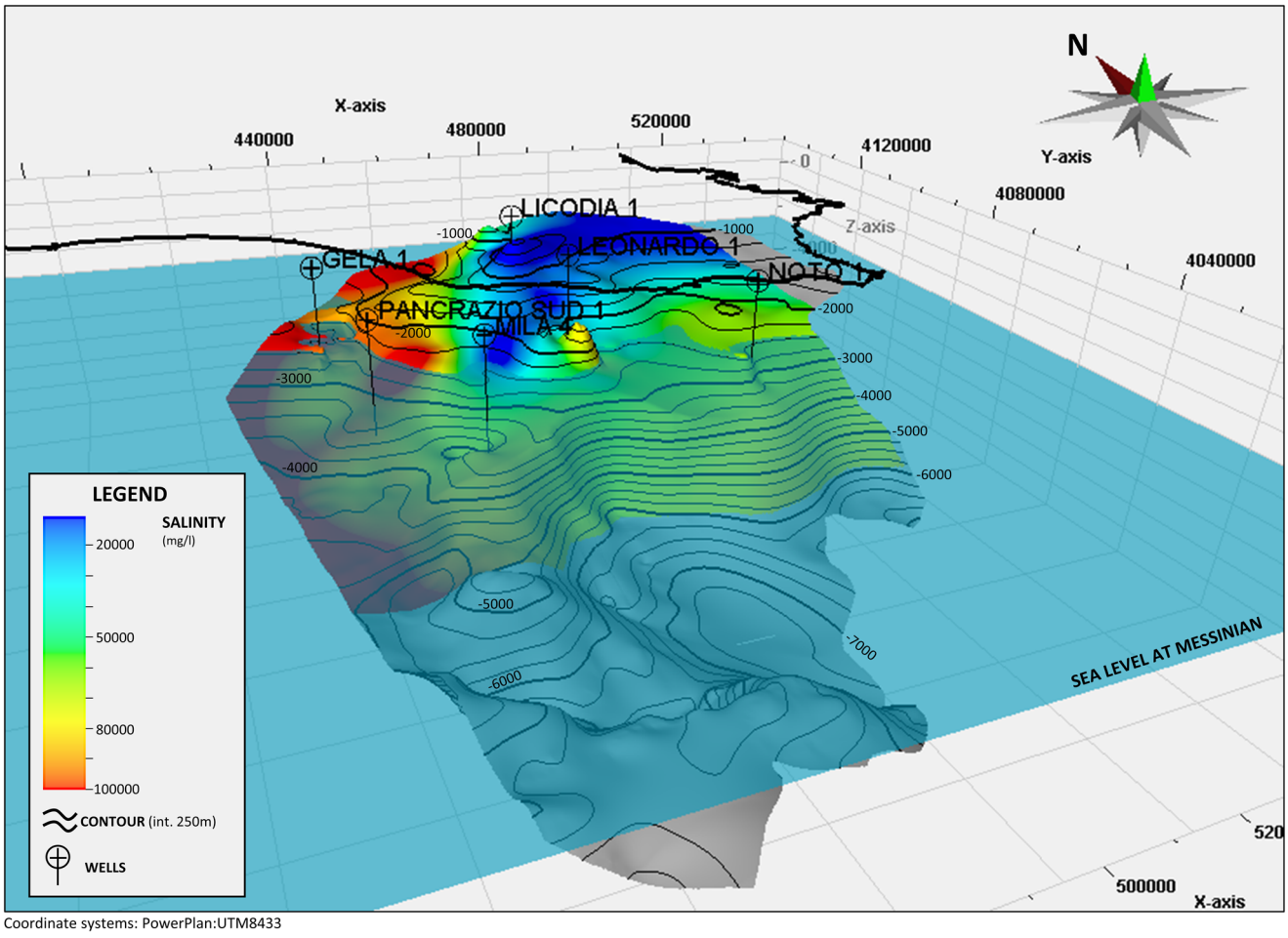

Fig. 7 3D structural/groundwater salinity map of the Gela fm. at Messinian time. 3D view of the groundwater salinity distribution of the Gela Fm. draped over its structural depth map reconstructed at Messinian time (5.97 Ma). Sea-level, at Messinian time, is interpreted to be at the base of the deepest freshened groundwater at −2400 m.

from[45,46]. Elsewhere, to the south, the Gela Fm. carbonates are sealed and confined by the Streppenosa shaly formation, while to the west and to the north it is deeply buried below the orogen front.

In our hypothesis, this direct connection along a basal section of the Malta Escarpment has resulted in a dramatic increase of the hydraulic head during the MSC, allowing the infiltration and mixing of topographically-driven meteoric freshwater deep into the Gela Fm. and possibly also draining out saline formation water from the Gela Fm. into the Mediterranean Sea.

In order to explain how the freshened groundwater hosted by the Gela Fm. has been retained to the present day (as demonstrated by good data), during and after the post-MSC sea-level rise, we consider that the extremely rapid post-MSC sea-level rise[47] eliminated the topographic gradient responsible for the deep invasion of meteoric waters and, as a consequence, deactivated the whole mechanism and pressure differentials. Indeed, groundwater systems are slow to adapt to the reconfiguration of the hydrological conditions[3], and such low-salinity water occurrences likely represent relict flow systems that sequestered fresh water under different morphology and sea-level conditions (palaeo-groundwater as per[3,48]).

Moreover, it is possible that during the MSC time, the deposition of hemipelagic shales and evaporites could have sealed that connection along the Malta Escarpment, preventing the entry of sea waters back into the Gela Fm. Finally, it is likely that a direct fault/fracture-related connection still exists between the deep Gela Fm. and the shallow aquifers of the Ragusa Fm., which is recharged by meteoric waters and hence could still provide an active hydraulic load, supporting the preservation of the deep fresh/brackish waters in the Gela aquifer.

The inferred value of 2400 m for the MSC sea-level drawdown is still characterized by uncertainties. On one hand, the value actually corresponds to the deepest part of the groundwater body, and the sea level could have actually also been shallower than that[49]. On the other, the inferred MSC sea level could have been deeper, because some of the groundwater could have undergone salinization.

With regards to the deep hypersaline groundwater (Fig. 5), this could have originated from the Middle/Lower Triassic deposits below the Gela Fm., which are known to be rich in evaporites[50]. We surmise that this deeper groundwater system is dominated by geothermal circulation, which involves the regional circulation of groundwater due to thermally induced buoyancy[40,51]. The present-day regional geothermal gradient, based on well data[24,52], is 25–35 C°/km in both the offshore/onshore domain in the upper 2 km, and it increases in the deeper section. This, combined with the proximity of colder deep water at the base of the Malta Escarpment, provides suitable conditions for geothermal convection[39].

Our study demonstrates that the main factors driving freshened groundwater recharge deep into the Gela Fm. include: (i) the presence of a shallow, outcropping fractured aquifer (Ragusa Fm.), which was able to capture and transfer meteoric water; (ii) a main transtensional fault/fracture system, which acted as a conduit of the meteoric waters from the shallow (Ragusa Fm.) to

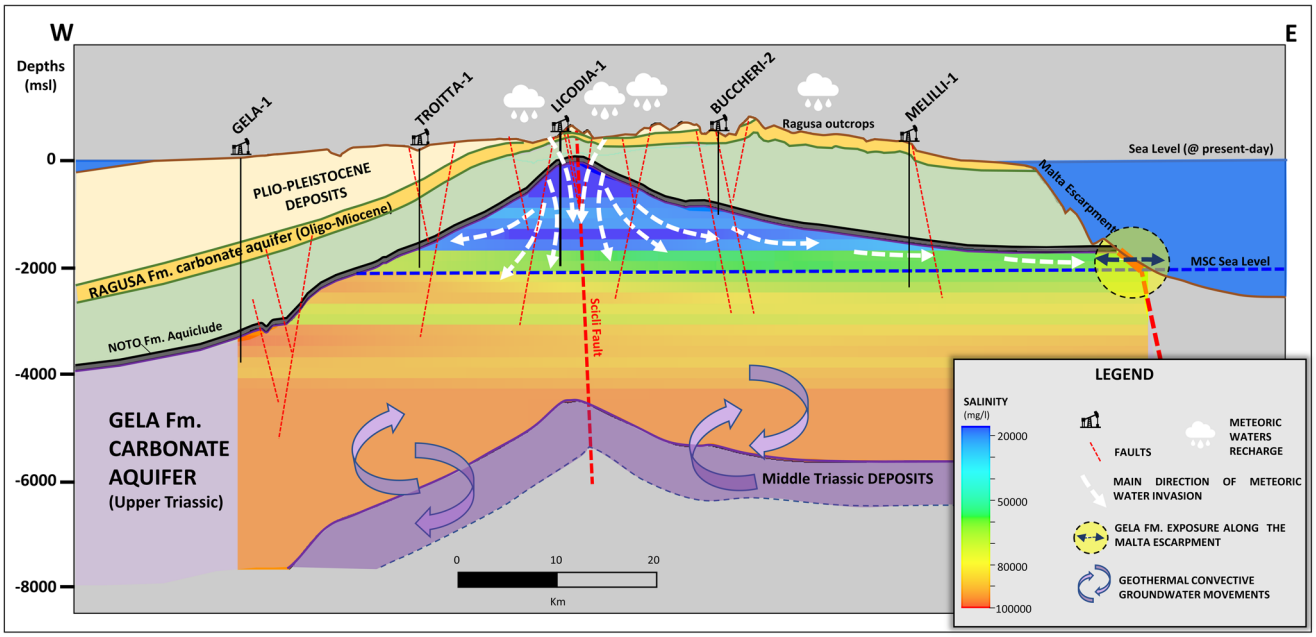

Fig. 8 Gela aquifer conceptual model. Conceptual model proposed for the deep groundwater circulation system within the Gela Fm. aquifer.

deep aquifer (Gela Fm.); and (iii) the MSC sea-level drawdown which exerted a fundamental control on deep freshened groundwater emplacement in the area, by creating the hydraulic heads that drove the meteoric waters to >2000 m below present sea-level (Fig. 8).

In summary, we explain the overall deep groundwater system hosted in the Gela Fm. (Fig. 8) as a combination of a shallower fluid circulation system, driven by the topographic head of meteoric waters invading the Gela Fm. during the MSC sea-level drawdown, and a deeper fluid circulation system, dominated by geothermal convection and buoyancy forces and characterized by hyper-saline groundwater sourced from evaporites.

The outcomes of our study are of interest because they can provide a regional case history to understand how the 3D geometry of a carbonate platform influences deep fluid circulation, especially during sea-level lowstands, and the model we propose for the emplacement of deep groundwater may also provide an explanation for coastal groundwater recorded at depths of >500 m below sea level in small Mediterranean islands (e.g., Kerkennah) or the Mediterranean seafloor, as these cannot be explained by recharge either at present or during Plio-Pleistocene glacial sea-level lowstands.

The discovery of such an extensive, preserved, and deep-freshened groundwater body has significant implications as an unconventional source of potable water, especially considering the numerous water-scarce areas along the Mediterranean coastlines (e.g., Morocco, Tunisia, Egypt, Lebanon, and Turkey[53]). Indeed, the geological setting and controlling factors in our study area occur elsewhere in the Mediterranean region, e.g., in the Adriatic Carbonate Platform and the Apulia Platform in Italy[54], in the Nara Platform in Tunisia, etc.[55] (and reference therein), where other extensive, deep freshened groundwater bodies may be hosted in carbonate aquifers. The technology to explore and utilize such deep groundwater bodies nowadays exists, making these potentially extensive groundwater resources available for utilization[1].

Data

This research has been based on a regional geological dataset, which includes public data and documents related to Oil and Gas exploration activities carried out in the last 50 years[23,24], and a collection of papers[25–29,32,34,35,43–46,50,56–58], both onshore and offshore of the study area. In total, 92 onshore and 30 offshore deep Oil&Gas wells have been analyzed in detail (Supplementary Fig. 1, Supplementary Table 1).

Methods

The methodological approach entailed a combination of well-established concepts from oil and gas exploration, reservoir engineering, geophysics, hydrogeology, and marine geology, dedicated to characterizing deep groundwater in terms of salinity, pressure, and 3D distribution at a regional scale.

3D geometric and structural reconstruction. Data were collected for the Gela Fm. over the whole study area, in terms of stratigraphic top, groundwater salinity, and pressures, and a summary sheet was generated (Supplementary Table 2).

The top of the Gela Fm. was mapped as per the following steps: (i) the structural top was obtained by interpolating and gridding the Gela Fm. top from good data (Supplementary Table 2); (ii) additional elements were created, such as the platform margin boundary and paleo-escarpment 3D geometry (Fig. 3), based on good data (while most of the wells were drilled over the platform area, some well instead investigated the platform margin and the adjacent basin), and published paleogeographic and facies distribution maps[32]; (iii) the base of the Gela Fm. was built and modeled considering a thickness of 4500 m in the carbonate platform setting (based on the Vizzini-1 well) while a minimum thickness of 500 m has been assumed below the Streppenosa Basin, considered as a remnant of the drowned older platform.

Groundwater pressure analysis. Formation water pressures were collected by analyzing wells Drill Stem Tests (DSTs) and Production Tests. Both tests involve an opening of the well valves to allow the production of formation fluids to flow into the well up to the surface, in order to allow direct fluid sampling and evaluation of well productivity. Some production tests are performed in open hole conditions (DST's) and are used in making completion decisions; others (Production Tests) are performed after the well is completed and generally involve routine measurements of fluids (oil, gas, and/or water production) under static

conditions. The test results can be used e.g., to determine reservoir properties, to assess the degree of damage or the need for stimulation, and to identify production and reservoir problems[59].

In order to assess the quality of pressure measurements, it was firstly important to evaluate the reliability of the executed tests. In particular the following was carefully considered:

- the pressures measured by the instrumentation in the well (hydrostatic pressure, flowing pressure, and shut-in pressure);
- the amount of produced fluid;
- the duration of each phase of the test.

In case: (i) the measured pressures (shut-in pressure) appear consistent with the depth of measurement and close to the hydrostatic regime; (ii) the amount of produced fluid was at least greater than the amount of existing drilling mud in the well and usually above 1 cubic meter; (iii) the duration of the test was reasonably long enough to allow formation fluids to flow into the well (usually at least one hour of test duration, depending on the type of rocks and their permeability), the test was considered reliable, and as a consequence also associate pressures measures. Vice versa, if one or more of the above conditions were not satisfied as a result of the tests, the test was not considered reliable.

As a result, based on DST and production test analysis, 25 onshore wells and 6 offshore wells tests provide good quality static pressure data at the Gela Fm.

Then, a depth calibration final step was done, as per the following: (i) a depth mid-point was calculated for each DSTs and Production Test to have the exact depth reference for the tested interval (which usually covers a range of about 30–60 m); (ii) each pressure measure (originally recorded at the measurement point in the well, known as gauge), was then corrected for depth (also considering the variation of fluids temperature and density with depth), since the pressure gauge was always placed above or close to the Gela Fm. top at a different and higher depth in respect of the tested interval.

Based on this detailed analysis, a final summary for all collected pressures was built (Supplementary Table 2).

Groundwater salinity analysis. Groundwater salinity data of the Gela Fm. were obtained through a detailed analysis of available Composite Logs and fluid tests. In all analyzed Composite Logs, the fluid salinity concentration is reported as g/l of chlorides, conventionally expressed as grams of NaCl per liter[60]. For convenience, in this work salinity is expressed in milligrams/liter (mg/l) of NaCl equivalent.

Once assessed the quality of DST and production tests (Methods—Groundwater pressure analysis), also the associated recorded salinity measures were considered reliable, as a direct measure of the formation water salinity, and vice versa. E.g., if the amount of fluid recovered during the test (DST or Production Test) is similar to the amount of existing drilling mud in the well, the salinity data could have recorded a low/lower salinity concentration due to the low salinity of the mud (which is always a water-based mud in the analyzed wells), and, as a consequence, the data could not be considered representative of the formation water salinity. In these cases, the test was not considered reliable and consequently, the salinity measurements were excluded from consideration.

As a result, reliable salinity data were obtained for 39 deep wells (33 onshore and 6 offshore), and a final summary was built (Supplementary Table 2). Groundwater Salinity measurements have been finally plotted with respect to their distance from the Gela Fm. top and with respect to their absolute depth, in order to investigate possible trends (Fig. 9).

3D groundwater model and volumetric calculations. The current 3D distribution of fresh, brackish, and saline waters was reconstructed and modeled in the subsurface for the Gela Fm. by developing a 3D detailed hydrogeological geocellular model, using Petrel (Fig. 6):

1. A 3D grid was used, according to the Petrel grid modeling tool (grid size of 500 m), using the Gela structural top (Supplementary Table 2) and base in order to obtain the bulk volume of the rock.
2. Groundwater salinity data, obtained from composite logs and fluid tests, were upscaled to populate the 3D geocellular model. Upscaling is the process of creating the cells that intersect the vertical profile of the wells by using the property derived from the well logs and averaging the values at the well locations according to the corresponding dimension of the 3D cells.
3. After having tested several layering solutions (e.g., "proportional to the structure", "following the base and the top", etc.) and layering thickness, a sub-horizontal layering was used with a cell thickness of 200 m, as it better was able to interpolate the groundwater salinity property.

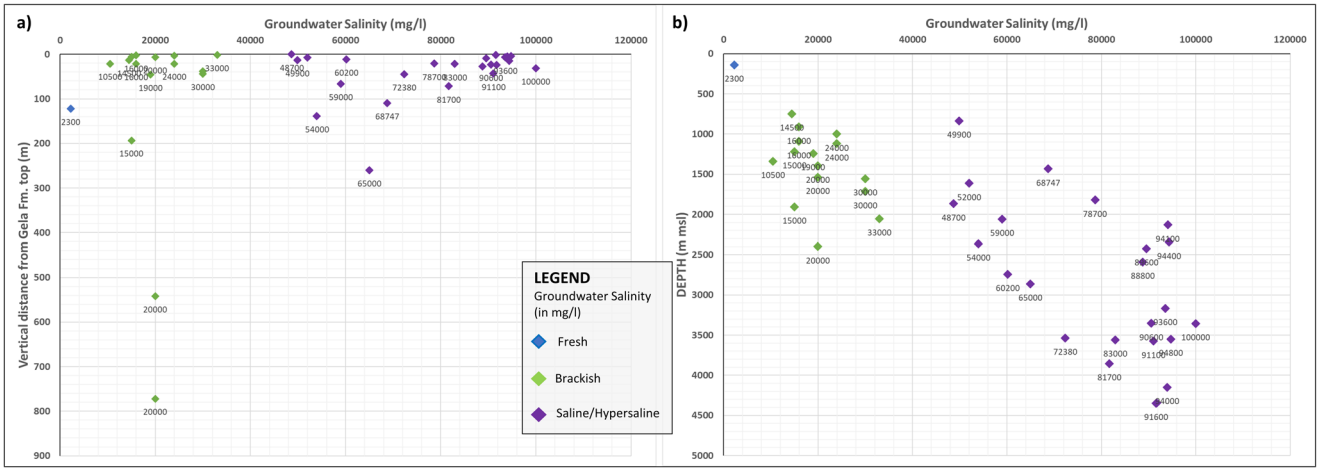

Fig. 9 Gela groundwater salinity graphs. a The groundwater salinity is shown with respect to the distance between the salinity measurement point from the Gela Fm. stratigraphic top. It can be observed that there is no correlation between the two parameters, suggesting that salinity values are not controlled by their stratigraphic position within the Gela Fm. **b** The groundwater salinity is shown with respect to depth. The graph shows a very good correlation between salinity measurements and depth.

4. Subsequently, the other cells of the structural model were populated through a deterministic kriging interpolation algorithm, using a petrophysical modeling tool.
5. Using the 3D Gela Fm. model, it was then possible to estimate the volumes of freshened groundwater (between 2000 and 20,000 mg/l) between the top (top of the Gela Fm.) and base (flat surface at −2100 m below present-day sea-level) of the freshened groundwater body, by using the calculated bulk volume of the rock and an average porosity value associate to fractures of 1%[61].

Back-reconstruction to the MSC. To assess the impact of the MSC sea-level drawdown on the distribution/characteristics of Gela Fm. groundwater, a back-reconstruction was performed at Upper Messinian time (5.97/5.33 Million years—Ma,[17,20,21,62,63]).

As a first step, it was considered that the Oligo-Miocene Ragusa Fm. is made of limestones and marly limestones deposited in a carbonate ramp setting, from neritic to pelagic conditions. To the East of the Hyblean plateau, equivalent deposits of the Ragusa Fm. are known as Monti Climiti and Palazzolo Fms.[58].

A. Based on facies and thickness distribution of the combined Ragusa/Monti Climiti Formations deposits, a hypothetical NE to SW prograding carbonate ramp (Fig. 10a) was then reconstructed at Langhian time (15.97 Ma[64]), on the basis of a classic depositional profile for a shallow marine Oligo-Miocene carbonate ramp[65], and using, as reference, the sea-level at Langhian time (which was about 40 m higher than present day[66]).
B. Comparing the top of the Ragusa/Monti Climiti Fms. at present-day with the reconstructed profile of the Ragusa/Monti Climiti carbonate ramp at Langhian time (15.97 Ma), it was possible to calculate the post-Langhian overall deformation experienced by the Ragusa/Mt.Climiti Fms. during this time period, which resulted in a vertical uplift over most of the area and local subsidence in the western sector of the study area (Fig. 10b).
C. Considering however that the active tectonic deformation affected the area only since Tortonian[27,67,68], and considering that the base of Tortonian is dated at 11.6 Ma[69], it was possible to calculate the average deformation rate, in meters per Ma, over the whole area (Fig. 10b, c).
D. Using the calculated average deformation rate, it was calculated the amount of displacement that occurred since the MSC (at Upper Messinian at 5.97 Ma), obtained by multiplying the average deformation rate times the Messinian age of 5.97 Ma (Fig. 10d).

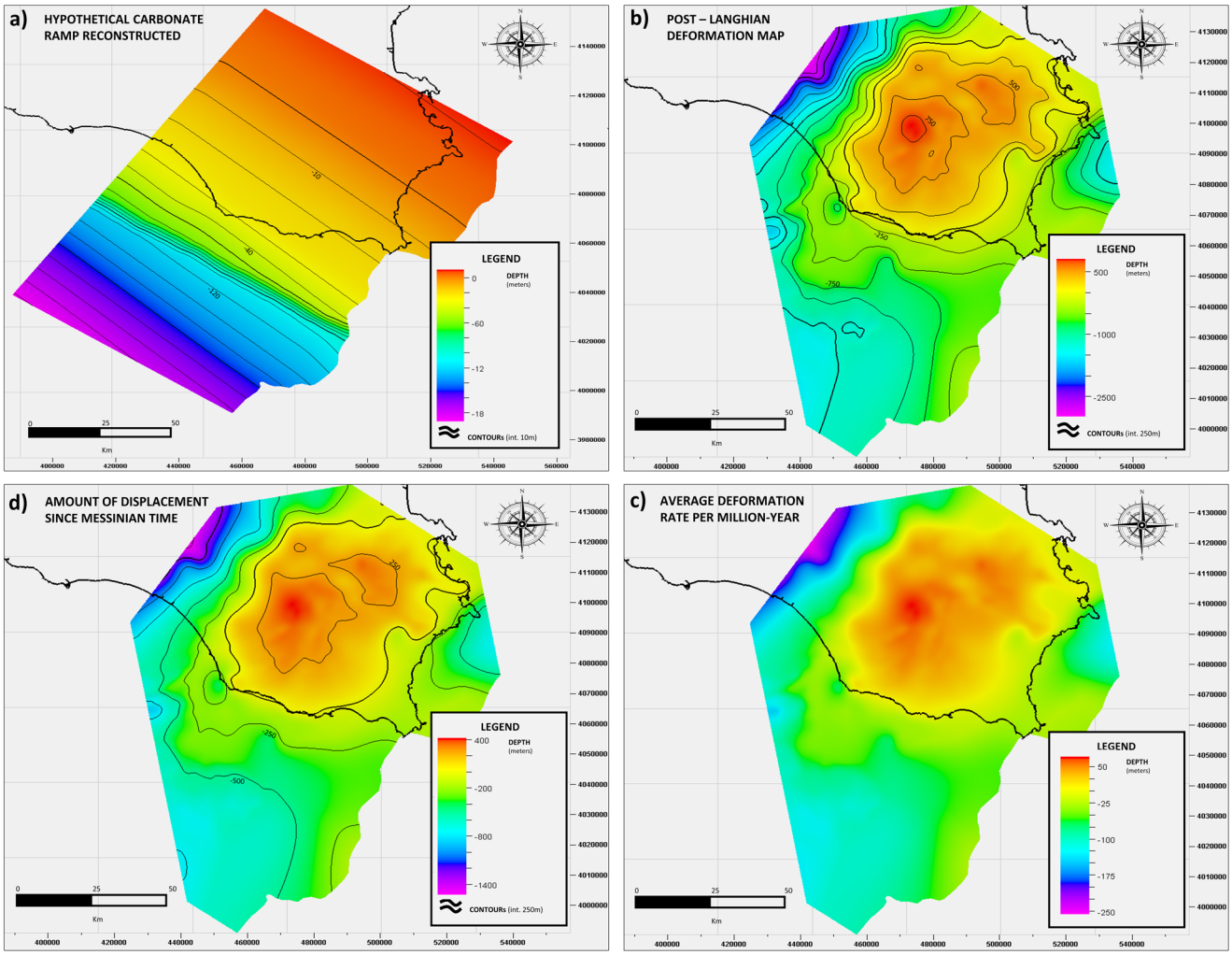

Coordinate systems: PowerPlan:UTM8433

Fig. 10 Back-reconstruction to the MSC. a Hypothetical Ragusa/Mt.Climiti Fms. carbonate ramp reconstructed at Langhian time 15.97 Ma. **b** Map of the post-Langhian total deformation experienced by the Ragusa/Mt.Climiti Fms. **c** Average deformation rate per million years. d Amount of displacement that occurred from the Messinian time (5.97 Ma) to present-day.

Once the work described was completed, it was considered that the same total deformation was experienced by the Ragusa/Monti Climiti Fms. (both uplift and subsidence) since Messinian was also experienced by the deeper Gela Fm. By applying the calculated amount of displacement to the present-day Gela Fm. structural top, it was hence finally possible to reconstruct the Gela Fm. structural top at Messinian (Fig. 7), in correspondence with the MSC, allowing to evaluation of the depth of −2400 m msl as an approximation of the depth reached by the MSC.

Data availability

This research has been based on a regional dataset, which includes public data and documents related to Oil & Gas exploration activities carried out in the last 50 years, extracted from the ViDEPI repository. ViDEPI (Visibility of petroleum exploration data in Italy), is an Italian publically accessible repository that includes well composites and documents concerning terminated, and therefore public, mining titles deposited since 1957 at UNMIG (the National Mining Office for Hydrocarbons and Georesources). It was built by the Ministry of Economic Development (MISE, Ministero dello sviluppo economico), in collaboration with the Italian Geological Society (SGI) and Assomineraria. Website URL: https://www.videpi.com/videpi/videpi.asp.

Received: 3 April 2023; Accepted: 27 October 2023;
Published online: 22 November 2023

References

1. UN-Water. *UN-water analytical brief on unconventional water resources. Geneva, Switzerland*. https://www.unwater.org/publications/un-water-analytical-brief-unconventional-water-resources-0 (2020).
2. Margat, J. & Van der Gun, J. *Groundwater around the world: a geographic synopsis. Crc Press*. https://doi.org/10.1201/b13977 (2013).
3. Post, V. E. et al. Offshore fresh groundwater reserves as a global phenomenon. *Nature* **504**, 71–78 (2013).
4. Van der Gun, J. *Large Aquifer Systems Around the World. The Groundwater Project, Guelph, Ontario, Canada*. https://doi.org/10.21083/978-1-77470-020-4 (2022).
5. Voss, C. I. & Soliman, S. M. The transboundary non-renewable Nubian Aquifer System of Chad, Egypt, Libya and Sudan: classical groundwater questions and parsimonious hydrogeologic analysis and modeling. *Hydrogeol. J.* **22**, 441 (2014).
6. Ruden, F. New perspectives on Saharan mega-aquifers: history, economic value and sustainability. *A Hist. Water Ser.* **3**, 16 (2016).
7. Siebert, C. et al. New tools for coherent information base for IWRM in arid regions: the upper mega aquifer system on the Arabian Peninsula. *Integr. Water Resour. Manag.* 85–106. https://doi.org/10.1007/978-3-319-25071-7_4 (Springer, Cham, 2016).
8. Habermehl, M. A. The evolving understanding of the Great Artesian Basin (Australia), from discovery to current hydrogeological interpretations. *Hydrogeol. J.* **28**, 13–36 (2020).
9. Moe, H., Ruden, F. & Gamache, M. Exploration and hydrogeological assessment of a deep coastal aquifer system in Tanzania. In *Proceedings of the Congress of the International Association of Hydrogeologists, Dubrovnik, Croatia* (Vol. 28) (2017).
10. Quiroga, E., Bertoni, C., Van goethem, M., Blazevic, L. A. & Ruden, F. A 3D geological model of the horn of Africa: new insights for hydrogeological simulations of deep groundwater systems. *J. Hydrol.* **42**, 101166 (2022).
11. Hathaway, J. C. et al. US Geological Survey Core Drilling on the Atlantic Shelf: geologic data were obtained at drill-core sites along the eastern US continental shelf and slope. *Science* **206**, 515–527 (1979).
12. Micallef, A. et al. Offshore freshened groundwater in continental margins. *Rev. Geophys.* **59**, e2020RG000706 (2021).
13. Ryan, W. B. Modeling the magnitude and timing of evaporative drawdown during the Messinian salinity crisis. *Stratigraphy* **5**, 227–243 (2008).
14. Roveri, M. et al. The Messinian Salinity Crisis: past and future of a great challenge for marine sciences. *Mar. Geol.* **352**, 25–58 (2014).
15. Meilijson, A. et al. Chronology with a pinch of salt: Integrated stratigraphy of Messinian evaporites in the deep Eastern Mediterranean reveals long-lasting halite deposition during Atlantic connectivity. *Earth Sci. Rev.* **194**, 374–398 (2019).
16. Lofi, J. *Seismic Atlas of the Messinian Salinity Crisis markers in the Mediterranean Sea-Volume 2. Soc. Géol. France* **181**, 1–72 (2014).
17. Hsü, K. J., Ryan, W. B. & Cita, M. B. Late Miocene desiccation of the Mediterranean. *Nature* **242**, 240–244 (1973).
18. Gargani, J. & Rigollet, C. Mediterranean sea-level variations during the Messinian 1115 salinity crisis. *Geophys. Res. Lett.* **34**, L10405 (2007).
19. Madof, A. S., Bertoni, C. & Lofi, J. Discovery of vast fluvial deposits provides evidence for drawdown during the late Miocene Messinian salinity crisis. *Geology* **47**, 171–174 (2019).
20. Ryan, W. B. Quantitative evaluation of the depth of the western Mediterranean before, during and after the Late Miocene salinity crisis. *Sedimentology* **23**(6), 791–813 (1976).
21. Roveri, M., Bassetti, M. A. & Lucchi, F. R. The Mediterranean Messinian salinity crisis: an Apennine foredeep perspective. *Sediment. Geol.* **140**, 201–214 (2001).
22. Lugli, S., Manzi, V., Roveri, M. & Schreiber, B. C. The deep record of the Messinian salinity crisis: evidence of a non-desiccated Mediterranean Sea. *Palaeogeogr. Palaeoclimatol. Palaeoecol.* **433**, 201–218 (2015).
23. Agip. *Acque dolci sotterranee. Inventario dei dati raccolti dall'Agip durante la ricerca di idrocarburi in Italia (dal 1971 al 1990)* (1994).
24. Videpi Project. Visibility of petroleum exploration data in Italy. MISE, Ministero dello sviluppo economico. https://www.videpi.com/videpi/videpi.asp (2015).
25. Patacca E., Scandone P. *Mesozoic paleotectonic evolution of the Ragusa zone (Southeastern Sicily)—Geologica Rom., 18—331–369, 67 fig., 1tab., 5tav. F. t., Roma*. (1979).
26. Cita, M. B. et al. Contribution to the geological exploration of the Malta Escarpment (eastern Mediterranean). *Riv. Ital. Paleontol. Stratigr.* **86**, 316–356 (1980).
27. Grasso, M. T. & Lentini, F. Sedimentary and tectonic evolution of the eastern Hyblean Plateau (southeastern Sicily) during late Cretaceous to Quaternary time. *Palaeogeogr. Palaeoclimatol. Palaeoecol.* **39**, 261–280 (1982).
28. Torelli, L., Grasso, M., Mazzoldi, G., Peis, D. & Gori, D. Cretaceous to Neogene structural evolution of the Lampedusa shelf (Pelagian Sea, Central Mediterranean). *Terra Nova* **7**, 200–212 (1995).
29. Grasso, M., Pedley, H. M., Maniscalco, R. & Ruggieri, R. Geological context and explanatory notes of the Carta geologica del settore centro-meridionale dell'altopiano Ibleo. *Mem. Soc. Geol. Ital.* **55**, 45–52 (2000).
30. Finetti, I. The CROP profiles across the Mediterranean sea (CROP MARE I and II). *Mem. Descr. Carta Geol. It* **62**, 171–184 (2003).
31. Yellin-Dror, A., Grasso, M., Ben-Avraham, Z. & Tibor, G. The subsidence history of the northern Hyblean plateau margin, southeastern Sicily. *Tectonophysics* **282**, 277–289 (1997).
32. Frixa, A., Bertamoni, M., Catrullo, D., Trincianti, E. & Miuccio, G. Late Norian-Hettangian paleogeography in the area between wells Noto 1 and Polpo 1 (S-E Sicily). *Mem. Soc. Geol. It.* **55**, 279–284 (2000).
33. Rocco, T. (1959). *11. Gela in Sicily, an Unusual Oil Field. In World Petroleum Congress (pp. WPC-8011). WPC.*
34. Casero, P. Structural setting of petroleum exploration plays in Italy. *Spec. Vol. Ital. Geol. Soc. IGC* **32**, 189–199 (2004).
35. Bertello, F. et al. From thrust-and-fold belt to foreland: hydrocarbon occurrences in Italy. In: (eds Vining, B. A. & Pickering, S. C.) *Petroleum Geology: From Mature Basins to New Frontiers. Proceedings of the 7th Petroleum Geology Conference*, 113–126 (2010).
36. INGV. *Piano di tutela delle acque della Sicilia—Bacino idrogeologico Monti iblei (R19IB). D.02.04*. (2007).
37. Catalano, S., Romagnoli, G. & Tortorici, G. Kinematics and dynamics of the Late Quaternary rift-flank deformation in the Hyblean Plateau (SE Sicily). *Tectonophysics* **486**, 1–14 (2010).
38. Cavallaro, D. et al. *Progetto SPOT-Sismicità Potenzialmente Innescabile Offshore e Tsunami: Report Integrato di Fine Progetto*. https://doi.org/10.5281/zenodo.3732887 (2020).
39. Tucker, M. E. & Wright, V. P. Diagenetic processes, products and environments. *Carbonate Sedimentol.* **314**, 364 (1990).
40. Sanford, W. E., Whitaker, F. F., Smart, P. L. & Jones, G. Numerical analysis of seawater circulation in carbonate platforms: I. Geothermal convection. *Am. J. Sci.* **298**, 801–828 (1998).
41. Micallef, A. et al. Geomorphic evolution of the Malta Escarpment and implications for the Messinian evaporative drawdown in the eastern Mediterranean Sea. *Geomorphology* **327**, 264–283 (2019).
42. Spatola, D. et al. A single-stage megaflood at the termination of the Messinian salinity crisis: Geophysical and modelling evidence from the eastern Mediterranean Basin. *Mar. Geol.* **430**, 106337 (2020).
43. Scandone, P. et al. Mesozoic and Cenozoic rocks from Malta escarpment (central Mediterranean). *AAPG Bull.* **65**, 1299–1319 (1981).
44. Casero, P., Cita, M. B., Croce, M. & De Micheli, A. Tentativo di interpretazione evolutiva della scarpata di Malta basata su dati geologici e geofisici. *Mem. Soc. Geol. It* **27**, 233–253 (1984).
45. Minelli, L. & Faccenna, C. Evolution of the Calabrian accretionary wedge (central Mediterranean). *Tectonics* **29**, TC4004 (*2010*).

46. Tugend, J., Chamot-Rooke, N., Arsenikos, S., Blanpied, C. & Frizon de lamotte, D. Geology of the Ionian Basin and margins: a key to the East Mediterranean geodynamics. *Tectonics* **38**, 2668–2702 (2019).
47. Garcia-Castellanos, D. et al. Catastrophic flood of the Mediterranean after the Messinian salinity crisis. *Nature* **462**, 778–781 (2009).
48. Edmunds, W. M., Milne, C. J. (eds.). Palaeowaters in Coastal Europe: evolution of groundwater since the late Pleistocene. palaeowaters in coastal Europe: evolution of groundwater since the late Pleistocene. *Geol. Soc. Lond.* https://doi.org/10.1144/gsl.sp.2001.189.01.02 (2001).
49. Carlston, C. W. An early American statement of the Badon Ghyben-Herzberg principle of static fresh-water-salt-water balance. *Am. J. Sci.* **261**(1), 88–91 (1963).
50. Martini, R. et al. Depositional environment and biofacies characterisation of the Triassic (Carnian to Rhaetian) carbonate succession of Punta Bassano (Marettimo Island, Sicily). *Facies* **53**, 389–400 (2007).
51. Caspard, E., Rudkiewicz, J. L., Eberli, G. P., Brosse, E. & Renard, M. Massive dolomitization of a Messinian reef in the Great Bahama Bank: a numerical modelling evaluation of Kohout geothermal convection. *Geofluids* **4**(1), 40–60 (2004).
52. Trumpy, E. & Manzella, A. Geothopica and the interactive analysis and visualization of the updated Italian National Geothermal Database. *Int. J. Appl. Earth Observ. Geoinf.* **54**, 28–37, (2017).
53. Hofste, R. W. et al. *Aqueduct 3.0: Updated decision-relevant global water risk indicators, World Resources Institute, Washington D.C.* https://www.wri.org/applications/aqueduct/water-risk-atlas (2019).
54. Nicolai, C., Gambini, R. Structural architecture of the Adria platform-and-basin system. In: (eds Patacca, E., Sartori, R., and Scandone, P.) (1990). *Tyrrhenian basin and Apennines. Kinematic Relations since Late Tortonian Times. Memorie della società Geologica Italiana*, vol. 45, 425–451 (2007).
55. Rusciadelli, G. & Shiner, P. Isolated carbonate platforms of the Mediterranean and their seismic expression—searching for a paradigm. *Lead. Edge* **37**(7), 492–501 (2018).
56. Jongsma, D., Van Hinte, J. E. & Woodside, J. M. Geologic structure and neotectonics of the North African continental margin south of Sicily. *Mar. Pet. Geol.* **2**, 156–179 (1985).
57. Max, M. D. & Colantoni, P. (eds.). *Geological development of the Sicilian-Tunisian Platform*. UNESCO, pp. 117–122 (1993).
58. Lentini, F. & Carbone, D. *Geologia della Sicilia—mem. Descr. Carta Geol. d'It. XCV, pp. 7–414 figg. 533, tabb. 5; Tavv. 5* (2014).
59. Lancaster, D. E. *Production Testing: Part 9. Production Engineering Methods—AAPG ME 10: Developmente Geology Reference Manual*, 474–476 (1992).
60. Agip. *Attività geologica di cantiere nella ricerca di idrocarburi. Agip, Direzione esplorazione idrocarburi.* (Ferrari, 1980).
61. Weber K. J. & Bakker M. *Fracture and vuggy porosity. SPE paper 10332.* https://doi.org/10.2118/10332-MS (1981).
62. Hsü, K. J. et al. History of the Mediterranean salinity crisis. *Nature* **267**, 399–403 (1977).
63. Rouchy, J. M. & Caruso, A. The Messinian salinity crisis in the Mediterranean basin: a reassessment of the data and an integrated scenario. *Sediment. Geol.* **188**, 35–67 (2006).
64. Pedley, H. M. Sedimentology and palaeoenvironment of the southeast Sicilian Tertiary platform carbonates. *Sediment. Geol.* **28**, 273–291 (1981).
65. Pomar, L., Mateu-Vicens, G., Morsilli, M. & Brandano, M. Carbonate ramp evolution during the late Oligocene (Chattian), Salento Peninsula, southern Italy. *Palaeogeogr. Palaeoclimatol. Palaeoecol.* **404**, 109–132 (2014).
66. Cornacchia, I., Brandano, M. & Agostini, S. Miocene paleoceanographic evolution of the Mediterranean area and carbonate production changes: a review. *Earth Sci. Rev.* **221**, 103785 (2021).
67. Finetti, I. R. et al. Geological outline of Sicily and lithospheric tectono-dynamics of its Tyrrhenian margin from new CROP seismic data. CROP Project: deep seismic exploration of the central Mediterranean and Italy, 319–375 (2005).
68. Lentini, F. & Carbone, S. *Ricostruzione paleogeografica e geodinamica della Sicilia sulla base dei dati geologici e geofisici. Rendiconti online sgi.* 1-Note Brevi, s, 95-97, 1 tab (2008).
69. Hilgen, F. et al. The global boundary stratotype section and point (GSSP) of the Tortonian stage (Upper Miocene) at Monte Dei Corvi. *Epis. J. Int. Geosci.* **28**, 6–17 (2005).

Acknowledgements

This work was supported by Marie Skłodowska-Curie grant funding under the umbrella of "Horizon 2020—Research and Innovation Framework Program 2020", to Lorenzo Lipparini and the University of Malta (Topographically-driven fresh groundwater flow in offshore carbonate platforms—OFF-GROUND project"—Grant Agreement number: 101038076. Aaron Micallef is supported by the David and Lucile Packard Foundation. Andrea D'Ambrosio is gratefully acknowledged for his support and suggestions. Schlumberger is thanked for providing academic Petrel software licenses to the University of Malta and to the University of Rome "Roma Tre".

Author contributions

L.L.: Conception and design of study (hypothesis, objectives, approach). Data analyses and interpretation. Writing all parts of the paper. D.C.: Data analysis and interpretation. Writing substantive part of the paper. R.B.: Support to data analysis and interpretation. Support to the conception and design of the study (hypothesis, objectives, approach). A.M.: Conception and design of study (hypothesis, objectives, approach). Significant and critical revision of the paper; supervision of the project that gave rise to the paper.

Competing interests

The authors declare no competing interests.

Additional information

Supplementary information The online version contains supplementary material available at https://doi.org/10.1038/s43247-023-01077-w.

Correspondence and requests for materials should be addressed to Lorenzo Lipparini.

Peer review information *Communications Earth & Environment* thanks Christian Siebert, Antonio Caruso, and the other, anonymous, reviewer(s) for their contribution to the peer review of this work. Primary Handling Editor: Joe Aslin. Peer reviewer reports are available.

Reprints and permission information is available at http://www.nature.com/reprints

Publisher's note Springer Nature remains neutral with regard to jurisdictional claims in published maps and institutional affiliations.